

CONFERENCE PRE-PRINT

PERTURBATED MAGNETIC FIELD THRESHOLD OF EDGE COHERENT OSCILLATION DURING ELM MITIGATION BY N=1 AND 2 RMPS

*Progress of ELM Control Experiments with RMP in HL-3 Tokamak*¹T. F. SUN, ¹YI LIU, ¹X. Q. JI, ^{1,2}B. T. CUI, ¹G. Z. HAO, ¹R. KE, ¹J.M. GAO, ¹N. WU, ¹S. WANG, ¹J. Q. XU, ¹A. WANG, ¹M. Y. HE and ¹Y. X. FENG¹Southwestern Institute of Physics, Chengdu 610041 China²Department of Engineering Physics, Tsinghua University, Beijing 100084 China

Email: suntf@swip.ac.cn

Abstract

The reference scenario for ITER is H-mode, the divertor energy flux density below 0.5MJ/m^2 ; The ELM frequency scales as $f_{\text{ELM}} \propto I_p^{-1.8}$ in the ITER baseline $Q \sim 10$ scenario, plasma current $I_p = 15\text{MA}$. Without control, natural $f_{\text{ELM}} \sim 1$ Hz with each ELM having $W_{\text{ELM}} \sim 20\text{MJ}$ must vary from $f_{\text{ELM}} \sim 7\text{Hz}$ for $I_p = 5\text{MA}$. RMP decreases the ELM amplitude and keep high current discharge has shown the different region of collisionalities on different devices. The ELM control has achieve with $n = 1$ and $n = 2$ RMP on HL-3 tokamak. The $n = 1$ RMP is produced by 2×4 coil array and experimentally determined access condition in terms of pedestal collisionality (ν_e^*) versus pedestal density as a fraction of the Greenwald density (n_e / n_{GW}) for mitigation of type I ELMs. The collisional region of type-I ELM mitigation with the $n=1$ RMP shows relatively wide range on HL-3 and the access condition is near the K-STAR access condition with $n = 1$. However, some different features are observed when ELMs are controlled by $n = 2$ RMP. The $n=2$ RMP change type-I ELM to small(grassy) ELM with the increasing n_e induced by RMP during the H-mode discharge accompanying long live mode. In the meantime, the turbulence near the pedestal is reduced and the Da radiation is enhanced. Small or grassy ELM help the transport of energy and the control effect decrease when the collisionality become lower. An edge coherent oscillation (ECO) with a bursting feature was also observed in the steep-gradient pedestal region of the H-mode plasmas in HL-3 tokamak, where the type-I edge-localized modes (ELMs) were mitigated by application of the RMP. It was found that the ECO with frequency of about 1 kHz is located at the edge pedestal region, and is excited by three-wave interaction of turbulence enhanced by the RMP field through the change of electron density gradient in the pedestal region because of pump-out effect. The oscillation drives a significant outflow of particles as directly measured by probes, thus providing a channel for a nearly continuous extra particle transport across the pedestal during the ELM mitigation by RMP.

1. INTRODUCTION

The primary operating scenario for ITER is H-mode which help access high fusion gain burning plasma conditions [1]. However, strong gradient of the pressure profile in the edge pedestal region of the H-mode plasma can trigger large repetitive bursts called edge-localized modes (ELMs), which often produce high transient heat loads on the plasma facing components. Extrapolation from current measurements suggest that the maximum ELM energy flux that can be repetitively deposited is 0.5MJm^{-2} [2]. The ELM frequency scales as $f_{\text{ELM}} \propto I_p^{-1.8}$ in the ITER baseline $Q \sim 10$ scenario, plasma current $I_p = 15\text{MA}$. Without control, natural $f_{\text{ELM}} \sim 1$ Hz with each ELM having $W_{\text{ELM}} \sim 20\text{MJ}$ must vary from $f_{\text{ELM}} \sim 7\text{Hz}$ for $I_p = 5\text{MA}$ [3]. RMP decrease the ELM amplitude and keep high current discharge has shown the different region of collisionalities on different devices.

The ELM mitigation by applying an $n = 1$ compact in-vessel resonant magnetic perturbation (RMP) coils has been observed on HL-2A device. The ELM frequency was increased by a factor of 2 and the ELM amplitude decreased, leading to a reduced heat load on the divertor plates. Clear ELM mitigation is achieved in a q_{95} window with q_{95} value range 3.55-3.85, which is explained in terms of the edge-peeling response, based on toroidal single fluid resistive plasma model MARS-F code with different assumption of toroidal flows [4]. The simulation results using the CLTx code show the footprints of strongly distorted magnetic field lines on the divertors are consistent with the energy deposit spots in the experiment [5].

An edge coherent oscillation (ECO) with a bursting feature was observed in the steep-gradient pedestal region of the H-mode plasmas, where the type-I ELMs were mitigated by application of the $n = 1$ RMP. It was found that the ECO with frequency of about 2 kHz is located at the edge pedestal region, and is excited by three-wave

interaction of turbulence enhanced by the RMP field through the change of electron density gradient in the pedestal region because of pump-out effect. The oscillation providing a channel for a nearly continuous extra particle transport across the pedestal during the ELM mitigation by RMP. The RMP significantly enhances the power spectrum in the high frequency (50-150 kHz) range, whereas the peaked power spectrum around 100 kHz is substantially modified to a flat shape during the mitigation with ECO [6]. Nonlinear modelling of ELM mitigation, utilizing 3D magnetohydrodynamic (MHD) code JOEKE, demonstrates that strong mode coupling among toroidal Fourier harmonics allows redistribution of the magnetic energy, which explains the ELM mitigation with modifying the edge magnetic topology and characteristics of the edge transport. A threshold value of around 4.5 kAt RMP coil current required for achieving the ELM mitigation. Modelling results utilizing the quasi-linear initial-value code MARS Q reveal that the electron neoclassical toroidal viscosity (NTV) due to three dimensional fields plays the key role of density pump-out with reduction of both the plasma density and toroidal flow speed [7]. But the threshold makes the RMP mitigate ELMs successfully with different types of phenomenon, including ELMs with higher frequency, grassy ELMs, and mitigated ELMs with ECOs. Compared to the mitigated ELMs with ECOs, the RMP induced grassy-ELMs in HL-2A are irregular in size and frequency. the ECO perturbations are much smaller in amplitude and shorter in time than the grassy ELMs or Type-I ELMs. the averaged stored energy drop, caused by ECOs ($\sim 0.1\%$), is one order of magnitude smaller than that due to grassy ELMs ($\sim 2.1\%$). The latter is in the same order compared to that due to the mitigated ELMs ($\sim 2.8\%$). That means another RMP current threshold may exist for ELM mitigation. The ELM control has achieved with $n = 1$ and $n = 2$ RMP on HL-3 tokamak. ELM mitigation with ECO is found by $n=1$ and $n=2$ RMP.

In this paper, the results of the RMP threshold of ELM mitigation with ECO will be discussed in the paper. Section 2 describes the experiment set and basic phenomena of RMP control ELM on HL-3 device. In section 3 the access conditions that have been found to be required to achieve type I ELM mitigation on HL-3 device. In section 4 threshold of RMP current during ELM suppression/mitigation will be explored. Section 5 give a summary and proposes possible mechanism that could explain the observations.

2. PROGRESS OF ELM CONTROL EXPERIMENTS WITH RMP IN HL-3 TOKAMAK

2.1 Setup of RMP Coil on HL-3

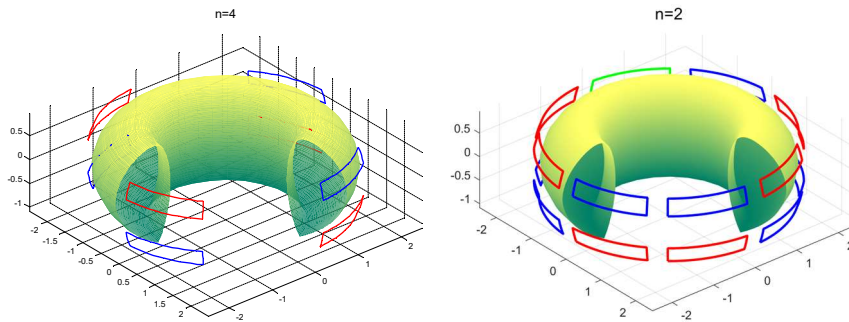


FIG. 1. The diagram of HL-3's $n=1$ and 2 RMP arrays.

A configuration of 16 RMP coils has been designed within the HL-3 VV, arranged in a toroidal \times poloidal layout of 8×2 . The cross-section shape of the HL-3 plasma region is D-shaped, and the layout of the RMP coils is illustrated in Fig. 1(a). The 16 coils are evenly divided into eight groups toroidally, and adjacent coils are spaced about 45° apart toroidally. RMP coil has a toroidal cover ratio of 80 %, and each coil can cover a 36 toroidal angle. Two rows of coils are symmetrically positioned above and below windows within the low field side (LFS) of the mid-plane, separated by approximately 73° poloidally. Installing the RMP coils inside the VV provides the benefit of reducing the duration for which the perturbed magnetic field penetrates the VV walls. Furthermore, being near the plasma offers the advantage of minimizing the required number of RMP coil turns, thereby conserving supplied power. The designated perturbed field (δB) is oriented towards the plasma as positive, indicated by the red current flow direction, with the current defined as '+', as shown in Fig. 2(a). Otherwise, indicated by the blue current flow direction, it is defined as '-'. Each coil is designed as a curved rectangle, with dimensions of approximately around 1552 mm \times 260 mm. Each coil can be individually controlled for the direction of current, allowing it to be set to one of three modes: positive connection, negative connection, or disconnection. The spectrum and amplitude of the RMP field are tuned by altering the coil's phase difference, denoted by $\delta\theta$. By changing the direction of the current in any coil, the phase can be adjusted to any desired value.

Typically, upper and lower rows of coil phase difference, employ 'odd' or 'even' connections. If the current of the coils in the upper and lower rows are the same, the phase difference is 0° , referred to as an 'even' connection. Conversely, if the current of the upper and lower row coils are completely opposite, the phase difference is 180° , known as an 'odd' connection. As exemplified in Fig. 2(a), it's a coil-even connection where are configured as '+-+-+-. Fig. 2(b) is an example of using 8 coils referred to as a coil-odd connection. The gray coils in the figure indicate disconnected. In addition to the 'odd' or 'even' mode, alternative other phase differences can also be achieved between the upper and lower coil rows, although these configurations are not commonly used in experiments. The 8×2 layout can produce a dominant magnetic perturbation spectrum with $n = 1, 2$, and 4. High n results in maximal edge disruption.

2.2 ELM mitigation with $n=1$ RMP

During ELM H-mode, $I_{RMP} n=1$ dominant spectrum varies from 8 kAt to 4.5 kAt step by step. RMP control ELM following 3 stage: ELM is mitigated firstly, and then the plasma exits the H mode with ne pumpout. In the last ne increases when I_{RMP} decreases and access H mode again after RMP. The threshold of mitigation is lower than 8 kAt. The toroidal magnetic field B_t change from 1T to 1.5T to scan the q_{95} window of ELM mitigation.

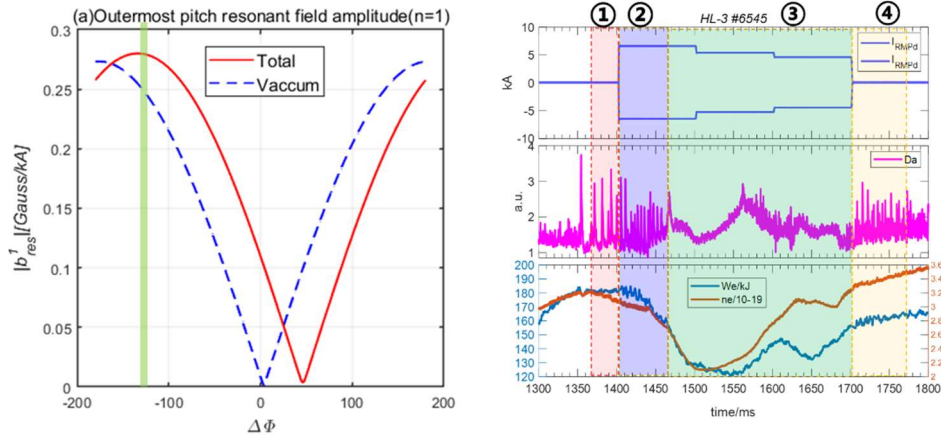


FIG.2. In the new machine HL-3 tokamak, the ELM control experiment is carried out with $n = 1$ RMP. The new result shows the process of the RMP making the ELM mitigated firstly and then induce H-L transition.

2.3 ELM mitigation with $n=2$ RMP

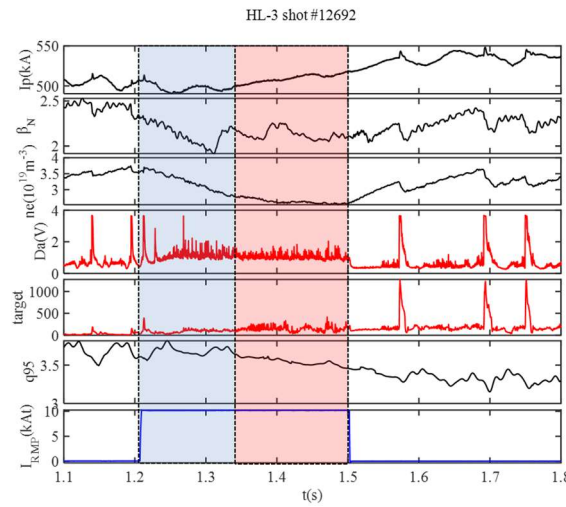


FIG.3. In the new machine HL-3 tokamak, the ELM control experiment is carried out with $n = 2$ RMP. The new result shows the process of the RMP making the ELM mitigated accompanying long live mode.

In this latest round of experiments, the RMP coils system set up as an odd connection where configured as '+ + - - + + 0 -' up-array and '+ + - - + + - -' down array with a dominant $n=2$ component, was a successful realization of ELM mitigation on the HL-3. Experimental results shown in this paper were obtained in plasmas with $B_t \sim 1.13$ T, $I_p \sim 500$ kA, line-average density $n_e \sim (1.9-3.5) \times 10^{20} \text{ m}^{-3}$, and safety factor at 95 % of equilibrium poloidal flux $q_{95} \sim 3.65$. A typical discharge with an ELM mitigation process is illustrated in figure 3, where the vertical sequence represents the plasma current, normalized ratio of β , deuterium alpha signal, deuterium alpha signal in target, q_{95} , and RMP coil current. The RMP is introduced at 1.2 s, and then $n=2$ perturbed field mitigate the ELM firstly with pump-outed n_e and then change ELM to small(grassy) ELM with the stable n_e .

3. ACCESS CONDITIONS FOR ELM CONTROL AT DIFFERENT PEDESTAL COLLISIONALITIES BY RMP

3.1 ACCESS CONDITIONS with $n=1$ RMP

The toroidal magnetic field B_t change from 1 T to 1.5 T to scan the q_{95} window of ELM mitigation. Through stored energy loss ΔW ELM statistics a wide q_{95} range of ELM mitigation with $n=1$ RMP is found through scanning I_p . The figure 4 shows ELM mitigation q_{95} is more than 4.2, and there is a quite wide range.

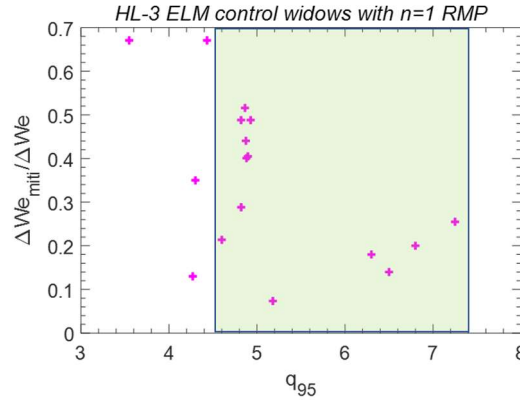


FIG. 5. The q_{95} range of ELM mitigation is more than 4.2.

The $n=1$ RMP experimentally determine access condition in terms of pedestal collisionality (v_e^*) [8] versus pedestal density as a fraction of the Greenwald density (n_e/n_{GW}) for mitigation of type I ELMs. The collisional region of type-I ELM mitigation with the $n=1$ RMP shows relatively wide range ($v_e^* = 0.1 \sim 1$) on HL-3 and the access condition is near the K-STAR access condition with $n=1$ as shown in figure 5.

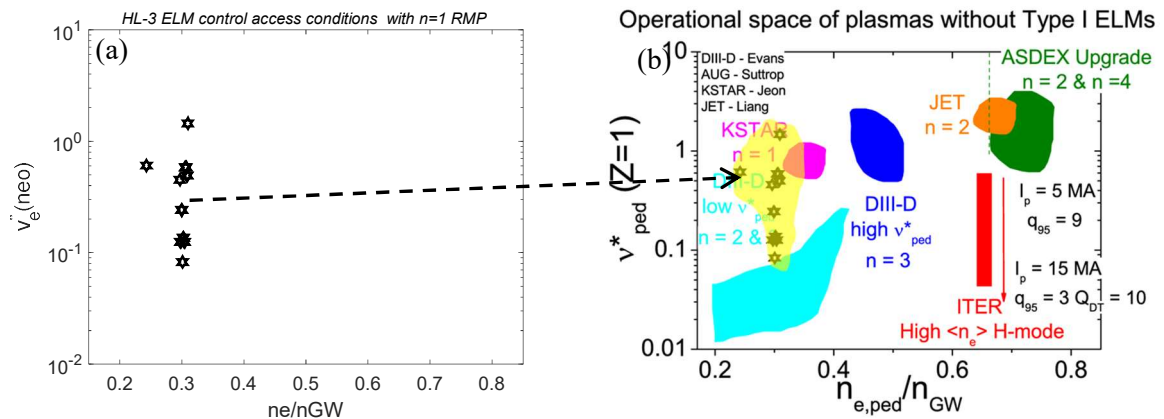


FIG. 6. Experimentally determined access condition in terms of pedestal collisionality (v_e^*) versus pedestal density as a fraction of the Greenwald density (n_e/n_{GW}): (a) The collisional region for mitigation of type I ELMs with RMP = 1; (b) comparison of access condition among different device, the yellow region is for HL-3.

3.2 ACCESS CONDITIONS with $n=2$ RMP

Some different features are observed when ELMs are controlled by $n = 2$ RMP on HL-3. The $n = 2$ RMP can control the ELM and change them to small(grassy) ELM with the pump-outed ne induced by RMP, and the saturated particle distribution on divertor target demonstrates the small or grassy ELM help the transport of energy and avoid high heat pulse of the big type-I ELM. The turbulence near the pedestal is reduced and the Da radiation is enhanced as shown in fig 7a. In the meantime, the core confine is influenced, and during the H-mode discharge the frequency of LLM decreases as shown in figure 7b.

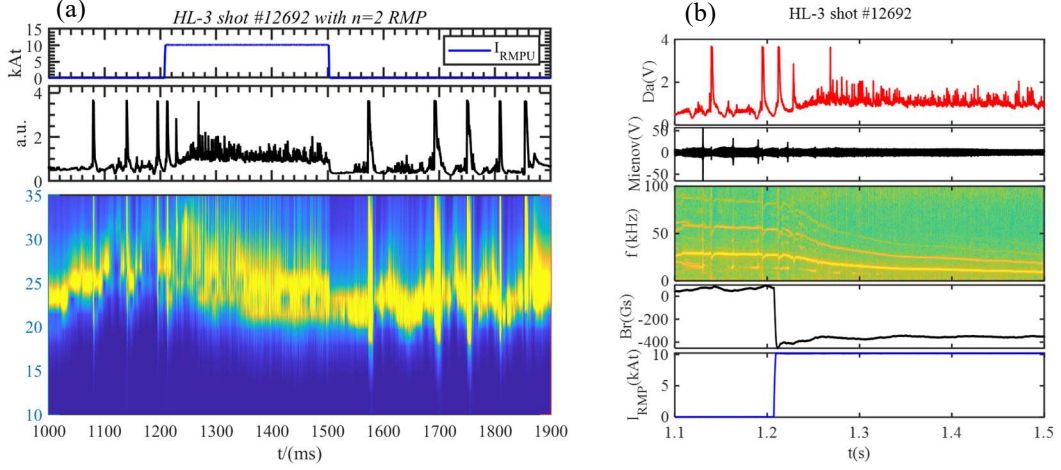


FIG. 7. RMP control ELM with $n=2$ RMP: (a) the saturated particle distribution on divertor target varies with time and RMP Control the ELM and change it to small ELM with enhanced Da radiation: the vertical sequence represents the plasma current, RMP coil current, deuterium alpha signal, and saturated particle distribution on divertor target; (b) the vertical sequence deuterium alpha signal, the spectrum of Soft-X signal, the perturbed magnetic field and RMP coil current.

Figure 8 shows another different features are observed when ELMs are controlled by $n = 2$ RMP on HL-3. There are two q_{95} widows of ELM control 3.7 and 5.2 through stored energy loss ΔW ELM statistics, which is found through scanning I_p from We loss. The mitigation effect decreases when the collisionality become lower as shown in the figure 8b.

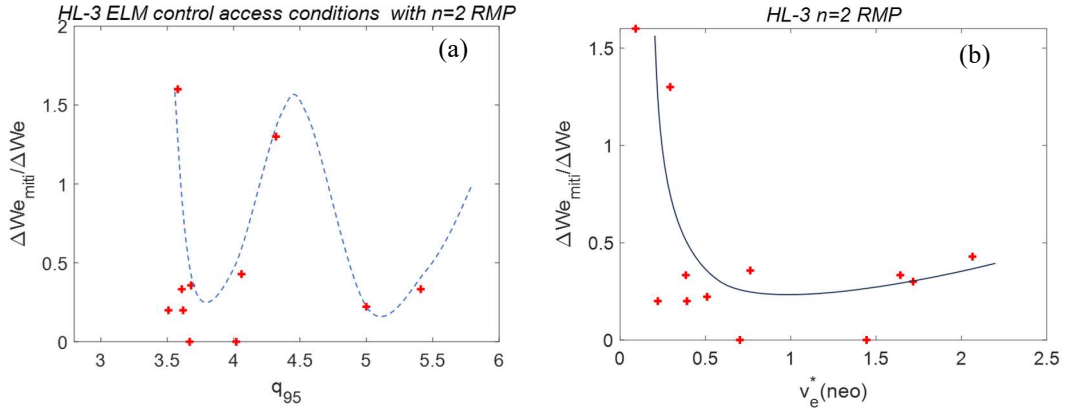


FIG. 8. (a) The q_{95} range of ELM mitigation with $n=2$ RMP through statistics of stored energy loss ΔW caused by ELM. (b) stored energy loss ΔW comparison between befor and after RMP changes with pedestal collisionality (v_e^*).

4. THRESHOLD OF RMP CURRENT DURING ELM SUPPRESSION/MITIGATION

4.1 The threshold of ELM mitigation with edge coherent oscillation (ECO) is found

ECO with the frequency near 1 kHz, in the pedestal region in the HL-3 tokamak persists continuously throughout the ELM mitigation phase. Within different RMP current, different types of mitigation have been observed, including ELMs with higher frequency, grassy ELMs, and mitigated ELMs with ECOs (as shown in Fig. 9). We emphasize that compared to the mitigated ELMs with ECOs, the RMP induced grassy-ELMs (with one example

shown in Fig. 7) in HL-3 are irregular in size and frequency. Moreover, as indicated by the expanded view on the right hand side panels of the figure, the ECO perturbations are much smaller in amplitude and shorter in time than the grassy ELMs or Type-I ELMs. Furthermore, as indicated by the comparison between ECOs with grassy-ELMs in the drop of the stored energy in Fig. 9 (c), the averaged stored energy drop, caused by ECOs ($\sim 0.1\%$), is one order of magnitude smaller than that due to grassy ELMs ($\sim 2.1\%$). The latter is in the same order compared to that due to the mitigated ELMs ($\sim 2.8\%$).

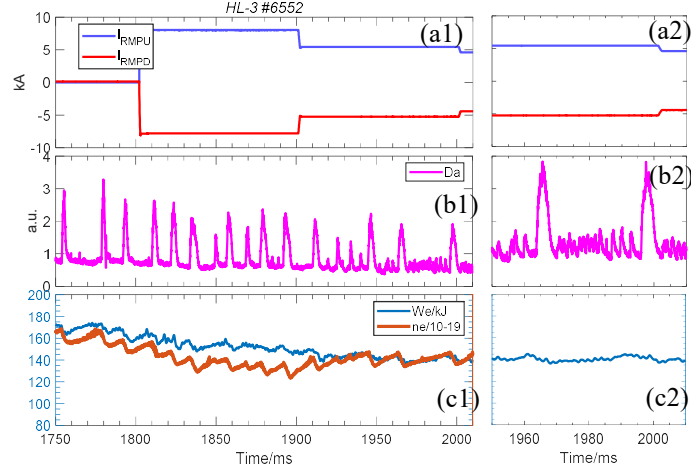


Figure 9. D_α signals for different RMP currents (8, 5.5, 4.5 kA) showing access to the RMP mitigated regime with ECO (a) RMP Current, (b) deuterium alpha signal, (c) stored energy and averaged electron density.

4.2 $n=1$ RMP CURRENT THRESHOLD EDGE COHERENT OSCILLATION

Figure 10 further plots the power spectrum of the density perturbation measured by the BES at different time slices[9]. It is evident that the RMP significantly enhances low power spectrum in the high frequency (600-800 kHz) range (light brown and orange), whereas the two peaked power spectrum around 630 kHz and 660 kHz are substantially modified to a flat shape during the mitigation with ECO (green). This suggests that there should be an energy transfer from the high frequency to the low frequency components during the nonlinear coupling process. The reason for enhanced energy cascading from high to low frequencies in ambient turbulence is not yet clear, it might be explained by the wave phase coupling theory [10] in which a clear physical picture of how large scale instability occurs through the spatial coupling of turbulences is given. Nevertheless, the results presented here reveal a possible mechanism of ECO excitation via three-wave interaction of turbulence enhanced by RMP.

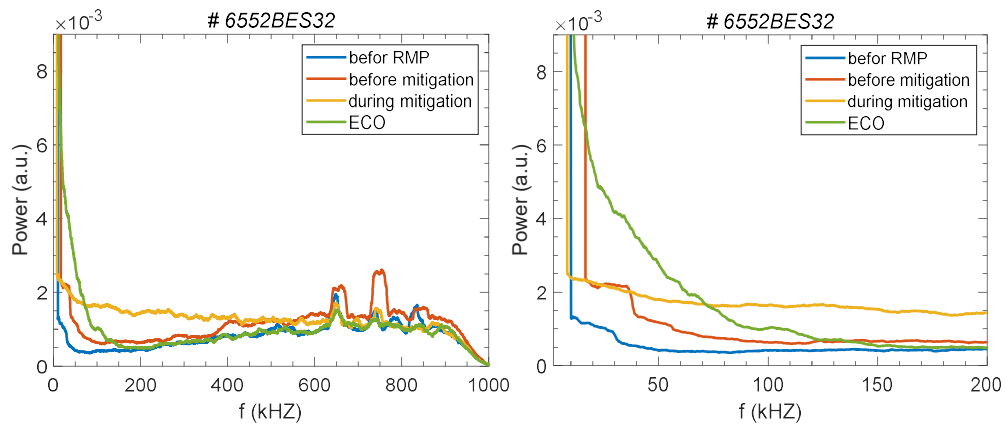


Figure 10. Power spectrum of density fluctuations in the range of 600-800kHz at different times, measured by BES in the pedestal top in HL-3 discharge 6552. Yellow and purple curves denote cases with and without mitigation during the application of RMP, respectively. The blue curves denote the case before RMP as a reference.

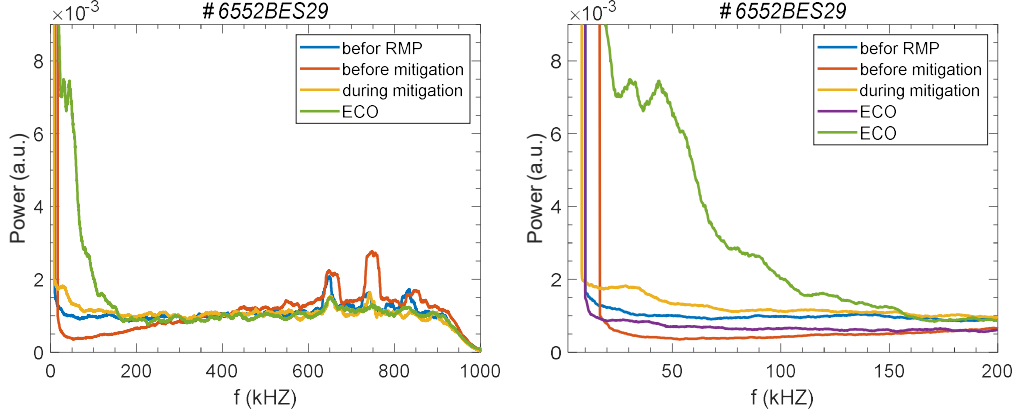


Figure 10. Power spectrum of density fluctuations in the range of 600-800kHz at different times, measured by BES in the pedestal bottom in HL-3 discharge 6552. Yellow and purple curves denote cases with and without mitigation during the application of RMP, respectively. The blue curves denote the case before RMP as a reference.

5. SUMMARY AND DISCUSSION

The ELM control has been achieved with $n = 1$ and $n = 2$ RMP on HL-3 tokamak. The $n = 1$ RMP is produced by 2×4 coil array and experimentally determined access condition in terms of pedestal collisionality versus pedestal density as a fraction of the Greenwald density (n_e / n_{GW}) for mitigation of type I ELMs. The collisional region of type-I ELM mitigation with the $n=1$ RMP shows relatively wide range on HL-3 and the access condition is near the DIII-D access condition with $n = 3$. Meanwhile, a wide q_{95} range of ELM mitigation with $n = 1$ RMP is found, which is more than 4.2. However, some different features are observed when ELMs are controlled by $n = 2$ RMP on HL-3. There are two q_{95} windows of ELM control 3.7 and 5.2 through stored energy loss ΔW ELM statistics, which is found through scanning I_p from We loss. The $n=2$ RMP can control the ELM and change them to small (grassy) ELM with the increasing n_e induced by RMP during the H-mode discharge accompanying long live mode. Small or grassy ELM help the transport of energy and the control effect decrease when the collisionality becomes lower. However, the result cannot validate the effective control range of collisionality with $n = 2$ RMP on HL-3 like the result of the AUG[8], because there are not enough data statistics. So, the next plan more ELM control experiment with $n=2$ need to be supplemented. ELM H-mode control will be carried out under hybrid operation scenario with the higher RMP like $n=4.1$. The current (Magnetic field) threshold of ECO is less than 8kAt, which is excited by turbulence enhanced by the RMP field through the change of electron density gradient in the pedestal region because of pump-out effect.

ACKNOWLEDGEMENTS

Acknowledges—This work is supported by the National Magnetic Confinement Fusion Energy R&D Program (Nos. 2024YFE03010004, Nos. 2022YFE03060002, Nos. 2022YFE03060002, 2022YFE03020003 and 2019YFE03010002). The work is partly supported by the National Natural Science Foundation (No. 12435014, No. 11875234).

REFERENCES

- [1] Loarte A. et al 2014 *Nucl. Fusion* **54** 033007
- [2] Loarte A et al 2013 Plan for ELM mitigation on ITER ITER Technical Report No 1. C
- [3] A. Kirk, PPCF 55 (2013) 124003 (11pp)
- [4] Liu Y.Q. et al. (2017) *Physics of Plasmas* **24**, 056111
- [5] Wang X. et al. (2023) *Nucl. Fusion* **63** 096023
- [6] Sun T. F. et al. (2021) *Nucl. Fusion* **61** 036020 (8pp)
- [7] Zhang N. et al. (2023) *Nucl. Fusion* **63** 086019
- [8] Suttrop W. et al, *Nucl. Fusion* **58** (2018) 096031
- [9] Sauter O, 1999 *Phys. Plasmas* **6** 2834

- [10] Ke R. et al 2018 Rev. Sci. Instrum. **89** 10D122
- [11] Xu Y. et al 2006 Phys. Rev. Lett. **97** 165003